Electrothermal Stability of Magnetohydrodynamic Plasma under Two-Component Magnetic Field

Naoyuki Kayukawa*
Hokkaido University, Sapporo, Japan

Based on the concept of variational calculus, a general criterion for calculating a dispersion relation of electrothermal waves was derived for a weakly ionized magnetohydrodynamic (MHD) plasma near cold electrodes. The theory was applied to examine the plasma stability characteristics under two different applied magnetic field configurations, namely, the magnetic field with a uniform z component and that with reduced z and moderate y components. Critical conditions for formations of arc spots were compared between these two B-field configurations under electrical and thermal boundary conditions suitable to an open-cycle MHD generator electrode. It was shown that the plasma stability limits as well as the critical current density, which defines the condition of arcing, were significantly improved in the case of the two-component magnetic field shaped near the electrode region.

Introduction

WHEN the rate of joule heating in a weakly ionized magnetohydrodynamic (MHD) plasma exceeds that of heat removal due to heat transfer, the thermal ionization of the gas is enhanced and the electrical current constricts further to deposit a higher joule heat. This type of electrothermal ionization instability occurs locally near an electrode surface with a distinct current density, beyond which the electrical conduction changes from the homogeneously diffused to the filamentary constricted arc discharge modes. In an open-cycle MHD power generator operated with a seeded combustion plasma, the current constriction appears generally near the cooled anode[1] at the current density of the order of 10^4 A/m^2. If the current density exceeds this critical value, arc spots are formed on the electrode, causing serious electrode arc damages.

Oliver[2] first formulated a linear perturbation theory to describe the mechanisms and characteristics of this arc transition phenomenon. Although the theory does not include the boundary conditions on the perturbed quantities, it explains that the stability limits decrease drastically with the increase in the Hall parameter and with the decrease in the wall temperature. Further, he considers that in almost all MHD generator conditions, the current conduction mode is in the unstable regime. Okazaki and his co-workers[3] investigated the same problem taking into account the boundary conditions suitable to an electrically and thermally conductive electrode. They also showed the strongly decreasing characteristics of the stability limits with the external magnetic field; the waves had tendencies to propagate in the direction of the magnetic field in the case of high Hall's parameters. Kon et al.[4] employed a variational formulation in order to include easily the boundary conditions and the magnetic field. They calculated the stability limits for thermally and electrically conductive, thermally nonconductive and electrically conductive, and thermally conductive and electrically nonconductive electrodes. In the last case, which corresponds to a cold electrode coated by an electrically resistant gaseous sublayer or by seed compounds, it was shown that the critical current density decreased more than one-fourth with the variation of Hall's parameter from zero to one and that the current constriction would be formed most easily in the case of the second electrode surface condition.

It may be possible to avoid the current constriction by restricting the current density below the critical value and the electrode deterioration by employing a highly durable electrode material such as platinum. However, the former reduces the power density and requires a large-sized generator volume to achieve high enthalpy efficiency, and the latter may be economically undesirable. Thus, the establishment of methods to insure higher stability limits for electrothermal instability under a strong magnetic field is still one of key problems in the design of a reliable and compact commercial MHD power generator.

In the present investigation, linear perturbation analyses were made for a thermally equilibrium magnetohydrodynamic plasma. The variational formulation used in Ref. 4 was generalized to take into account three components of both the current density and the electric field. The applied magnetic field was assumed to have two components, both of which were perpendicular to the plasma flow direction. The B-field component in parallel with the plane of electrode was assumed to be extremely reduced near the electrode, while its level at the core plasma region was kept about as high as in the conventional MHD generator with a uniform B-field having one component. Consequently, we assumed the existence of another component, which is perpendicular to the electrode. This type of magnetic field was introduced as a model for the B-field configuration near electrode walls in the shaped-B-field-configuration-type (SFC-type) MHD generator proposed by the present author.[5]

The general dispersion relation was used to calculate the stability limits for the initiation of the current constriction, which was quasi-normal to the electrode. The stability limits calculated in the SFC-type MHD generator with realistic magnetic field strength near the electrodes were compared with those predicted in the uniform B-field-configuration-type (UFC-type) MHD generator.

Fundamental Equations and Variational Formulation

Since the purpose of the present analysis is to clarify the dependence of the electrothermal stability characteristics upon the magnetic field and its configuration, as well as upon the

Received Dec. 11, 1984; revision received Aug. 30, 1985.

*Associate Professor, Department of Nuclear Engineering, School of Engineering.

Hall parameter in a weakly ionized MHD plasma, we assume a thermally and chemically equilibrium plasma and neglect very near-wall phenomena occurring in the range of Debye length, such as the space charge effect. We also assume the ionization equilibrium and a small magnetic Reynolds number. The fundamental equations to be used are the generalized Ohm's law without the ion slip and the electron pressure gradient, the conservation of the electric current, the equation for the irrotational electric field, and the equation of the energy balance between heat conduction and joule heating. We suppose a thin low-temperature and low-conductivity layer over an electrode with a current density of the order of $10^3 \sim 10^4$ A/m^2. Under this condition, the viscous dissipation and the radiative heat transfer in the energy equation can be neglected in comparison with the joule heating term. We consider the plasma stability under a prescribed flowfield condition, so that we need not to employ the equation of motion.

Under these assumptions, the linearized formulas of the fundamental equations for a perfect gaseous plasma can be written as follows:

$$\boldsymbol{J}_1 = \sigma_0 \boldsymbol{E}_1 - \mu_0 \boldsymbol{J}_1 \times \boldsymbol{B} + (\sigma_0 \sigma_T \epsilon_0 - \mu_0 \mu_T \boldsymbol{J}_0 \times \boldsymbol{B}) T_1 \tag{1}$$

$$\nabla \cdot \boldsymbol{J}_1 = 0 \tag{2}$$

$$\nabla \times \boldsymbol{E}_1 = 0 \tag{3}$$

$$\frac{\partial T_1}{\partial t} + \boldsymbol{V} \cdot \nabla T_1 + \rho_T (\boldsymbol{V} \cdot \nabla T_0) T_1 = \alpha_0 \nabla^2 T_1 + \frac{(2\boldsymbol{J}_0 \cdot \boldsymbol{J}_1 - J_0^2 \sigma_T T_1)}{\rho_0 C_p \sigma_0} \tag{4}$$

where $\boldsymbol{J}$, $\boldsymbol{E}$, $\boldsymbol{V}$, and T are, respectively, the current density, electric field, flow velocity, and plasma temperature, and $\epsilon = \boldsymbol{E} + \boldsymbol{V} \times \boldsymbol{B}$. Subscripts 0 and 1 refer to the unperturbed and the perturbed quantities. Here C_p, ρ, μ, and σ are the specific heat at constant pressure, mass density, electron mobility, and electrical conductivity, respectively. Also, $\sigma_T = \partial \ell n \sigma_0 / \partial T_0$, $\rho_T = \partial \ell n \rho_0 / \partial T_0$ and $\mu_T = \partial \ell n \mu_0 / \partial T_0$. The thermal diffusivity may consist of laminar and turbulent parts, i.e., $\alpha_0 = \alpha_\ell + \alpha_t$. The laminar thermal diffusivity is given by $\alpha_\ell = \kappa / \rho_0 C_p$ with κ the thermal conductivity and, after Clauser,[6] the turbulent thermal diffusivity in the case of unit Prandtl number can be evaluated approximately by $\alpha_t = 0.0188 V_\infty d$ with V_∞ the core flow velocity and d the displacement thickness. In Eqs. (1-4), perturbations in the flow velocity, magnetic field, and both thermal diffusivities are neglected.

We employ the coordinate system and a rectangular magnetohydrodynamic channel with segmented electrode configuration as shown in Fig. 1. Assuming that $\boldsymbol{V} = (V,0,0)$, $\boldsymbol{E} = (E_x, E_y, E_z)$, $\boldsymbol{J} = (J_x, J_y, J_z)$, and $\boldsymbol{B} = (0, B_y, B_z)$, the unperturbed equilibrium current density $\boldsymbol{J}_0$ is related to the electric field by

$$\boldsymbol{J}_0 = \frac{\sigma_0}{1 + \beta_y^2 + \beta_z^2} \begin{bmatrix} 1 & -\beta_z & \beta_y \\ \beta_z & 1 + \beta_y^2 & \beta_y \beta_z \\ -\beta_y & \beta_y \beta_z & 1 + \beta_z^2 \end{bmatrix} \epsilon_0 \tag{5}$$

where $\beta_y = \mu B_y$ and $\beta_z = \mu B_z$, the Hall parameters related to each magnetic field component.

Okazaki et al.[7] compared the results obtained by taking into account the steady-state temperature distribution in the direction normal to the electrodes with those calculated by a simplified boundary-layer model in which no temperature distribution was considered. They showed that, in case of a model having a thin low-conductivity layer with Saha equilibrium plasma, there existed little differences between the two models with regard to the fundamental features of the plasma stability, namely, the dependencies of the stability limits upon the wave number and the electrode surface temperature. It is reasonable to assume that this conclusion is adaptable in the present case without regard to the difference in the magnetic field configuration. Although the two magnetic field components are generally functions of both y and z coordinates, their spatial variation in the layer may not be so steep as that of the temperature. Thus, it may also be admissible to assume constant values for the magnetic field as well as the Hall parameters in the following calculations. Further, we neglect the mobility dependence upon the temperature for simplicity in what follows. The effects of varying the mobility have been considered by the present author in Ref. 8, where it is shown that the condition $\mu_T = 0$ introduces a slight underestimation of the stability limits.

With these assumptions and assuming plane wave type solutions for all of the perturbed parameters in Eqs. (1-4) and keeping the amplitude as unknown functions of y such as $\boldsymbol{J}_1 = \hat{\boldsymbol{J}}(y) \exp[i(\omega t - k_x x - k_z z)]$, and eliminating $\hat{E}(y)$, $\hat{J}_x(y)$, and $\hat{J}_z(y)$, we obtain the following set of ordinary differential equations with respect to the amplitude $\hat{J}_y(y)$ and $\hat{T}(y)$:

$$D^2 \hat{J}_y - iP_0 D\hat{J}_y - P_1 \hat{J}_y - iP_2 D\hat{T} + P_3 \hat{T} = 0 \tag{6}$$

$$D^2 \hat{T} - Q_1 \hat{T} + iQ_2 D\hat{J}_y + Q_3 \hat{J}_y = 0 \tag{7}$$

where $D = d/dy$, $i^2 = -1$, and P and Q are defined as

$$P_0 = \frac{2\beta_y \beta_z k_z}{(1 + \beta_y^2)}$$

$$P_1 = \frac{[k_x^2 + (1 + \beta_z^2) k_z^2]}{(1 + \beta_y^2)}$$

$$P_2 = \frac{[(a_x + \beta_y a_z) k_x - (\beta_y a_x - a_z) k_z]}{(1 + \beta_y^2)}$$

$$P_3 = \frac{[a_y k_x^2 + (\beta_z a_x + a_y) k_z^2 - \beta_z a_z k_z k_x]}{(1 + \beta_y^2)}$$

$$Q_1 = \frac{i\omega}{\alpha_0} - \frac{ik_x V}{\alpha_0} + k_x^2 + k_z^2 - \frac{(\gamma_1 k_x^2 + \gamma_2 k_z^2 + 2\gamma_3 k_x k_z)/(k_x^2 + k_z^2)}{(1 + \beta_y^2 + \beta_z^2)(\alpha_0 \rho_0 C_p \sigma_0 \sigma_T)}$$

$$Q_2 = \frac{2\gamma_4/(k_x^2 + k_z^2)}{(1 + \beta_y^2 + \beta_z^2)(\alpha_0 \rho_0 C_p \sigma_0 \sigma_T)}$$

$$Q_3 = \frac{2\gamma_5/(k_x^2 + k_z^2)}{(1 + \beta_y^2 + \beta_z^2)(\alpha_0 \rho_0 C_p \sigma_0 \sigma_T)}$$

with $a_x = \sigma_0 \sigma_T \epsilon_{0x}$, $a_y = \sigma_0 \sigma_T \epsilon_{0y}$, $a_z = \sigma_0 \sigma_T \epsilon_{0z}$, and γ defined by

$$\gamma_1 = -a_x^2 - (1 + \beta_y^2) a_y^2 + (1 + \beta_z^2) a_z^2$$

$$\gamma_2 = a_x^2 - (1 + \beta_y^2) a_y^2 - (1 + \beta_z^2) a_z^2 - 2\beta_z a_x a_y - 2\beta_y \beta_z a_y a_z + 2\beta_y a_z a_x$$

$$\gamma_3 = \beta_y a_x^2 - \beta_y a_z^2 - \beta_y \beta_z a_x a_y + \beta_z a_y a_z - (2 + \beta_z^2) a_z a_x$$

$$\gamma_4 = [-(1 + \beta_y^2)(a_x - \beta_z a_y) + \beta_y \beta_z^2 a_z] k_x^2 + (1 + \beta_y^2 + \beta_z^2) a_z k_z$$

$$\gamma_5 = [\beta_z a_x + (1 + \beta_y^2) a_y + \beta_y \beta_z a_z] k_x^2 + (1 + \beta_y^2 + \beta_z^2) a_y k_z^2 + \beta_z [-\beta_y a_x + \beta_y \beta_z a_y + (1 + \beta_z^2) a_z] k_x k_z$$

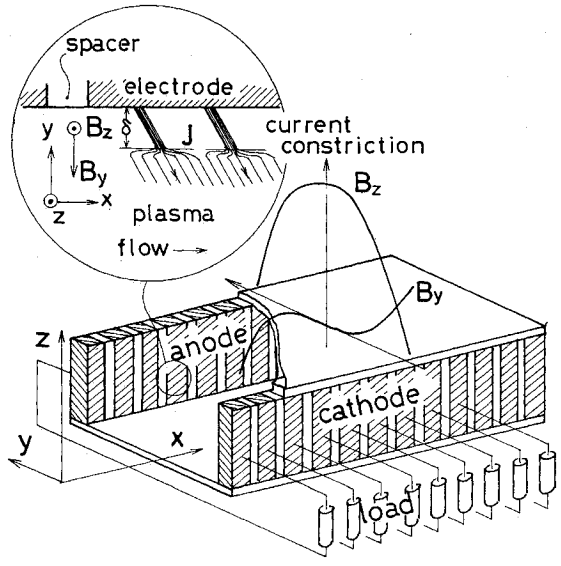

Fig. 1 Coordinate system of an MHD generator channel with the shaped B-field configuration and the current constriction model near the segmented anode wall.

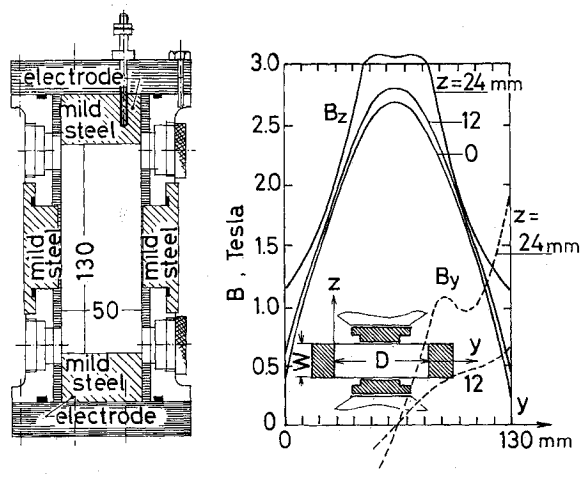

Fig. 2a Experimental SFC-type MHD channel with ferromagnetic walls and distribution of the two magnetic field components over the cross section.

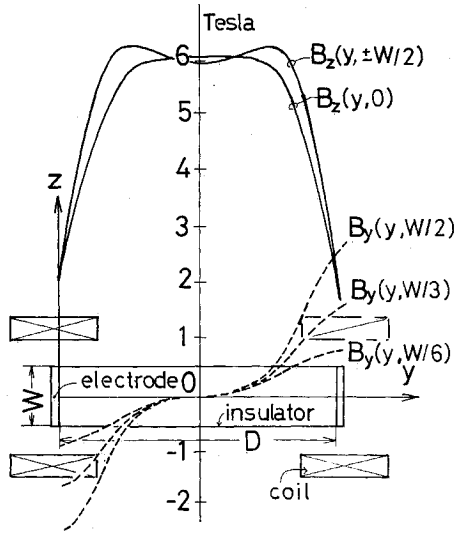

Fig. 2b Shaped B-field configuration designed by the racetrack-type superconducting coils.

Eliminating the temperature amplitude from Eqs. (6) and (7), we get

$$(D^4 - iP_0D^3 - Q_0D^2 - iR_0D + S_0)\hat{J}_y = 0 \tag{8}$$

where $Q_0 = P_1 + P_2Q_2 + Q_1$, $R_0 = P_3Q_2 - P_0Q_1 - P_2Q_3$, and $S_0 = P_1Q_1 - P_3Q_3$.

According to the variational calculus,[9] the Euler equation giving a minimum or an extreme of the action integral containing the highest nth order derivatives should take a form of the $2n$th order of ordinary differential equation. Because of this requirement, Eq. (8) must be operated with $D^4 - Q_0D^2 + S_0 + i(P_0D^3 + R_0D)$ to give the Euler equation with $n=4$. Then, the action integral $I[\hat{J}_y(y)]$ that gives just this Euler equation can be written formally as (see Appendix)

$$I(A_m, A_n) = \sum_{m=1}^{\infty}\sum_{n=1}^{\infty} A_m A_n \langle m|n\rangle \tag{9}$$

where A_m is constant coefficients of the assumed polynomial of appropriate functions $J_{ym}(y)$ that satisfy given boundary conditions at $y=0$ (wall surface) and $y=\delta$ (the edge of the perturbed plasma region). In Eq. (9), $\langle m|n\rangle$ is defined by

$$\begin{aligned}\langle m|n\rangle = \int_0^{\delta} [&D^4 J_{ym} D^4 J^*_{yn} - (P_0^2 - 2Q_0) D^3 J_{ym} D^3 J^*_{yn} \\ &+ (Q_0^2 + 2P_0R_0 + 2S_0) D^2 J_{ym} D^2 J^*_{yn} \\ &- (R_0^2 - 2Q_0S_0) DJ_{ym} DJ^*_{yn} + S_0^2 J_{ym} J^*_{yn}]\,dy\end{aligned} \tag{10}$$

where m is the constriction mode number and J^*_{yn} the complex conjugate of J_{ym}. Since the action integral must be extreme with respect to an assumed nontrivial solution $J_{ym}(y)$, it is required that $\partial I/\partial A_m = 0$. Therefore, we obtain m algebraic equations with respect to A_n, and the condition for the existence of nontrivial solution of A_n, that is,

$$\det\langle m|n\rangle = \begin{vmatrix} \langle 1|1\rangle & \langle 1|2\rangle & \cdots \\ \langle 2|1\rangle & \langle 2|2\rangle & \cdots \\ \vdots & \vdots & \ddots \end{vmatrix} = 0 \tag{11}$$

yields the desired dispersion relation for the electrothermal waves in an MHD plasma.

Calculation of the dispersion relation and stability limits can be carried out as follows. First, assume an appropriate polynomial function for the temperature amplitude $T_{ym}(y)$ that satisfies given boundary conditions at $y=0$ and $y=\delta$. Next, solve Eq. (6) to obtain $J_{ym}(y)$ and then $J^*_{yn}(y)$. Finally, perform the integration [Eq. (10)] and calculate the dispersion relation or the stability limits for Eq. (11).

Next, we apply the above general criterion to examine plasma stability characteristics near the segmented electrode wall under surface conditions that are typical in an open-cycle MHD generator.

Thermally Conductive and Electrically Nonconductive Electrodes

We first calculate the stability limits for the equilibrium current near an electrically nonconductive and thermally conductive surface. This condition may simulate a cooled noncoal slagging electrode coated by electrically resistive seed compounds. The appropriate boundary conditions to be imposed on the temperature and the current density amplitudes are

$$\hat{T}(0) = \hat{T}(\delta) = \hat{J}_y(0) = \hat{J}_y(\delta) = 0$$

Thus, we can assume the polynomial function for the temperature as

$$T_m(y) = A_m \sin(m\pi y/\delta) \tag{12}$$

We neglect the equilibrium electric fields parallel to the electrode: $\epsilon_{0x} = \epsilon_{0z} = 0$. This assumption may hold when the electrode surface resistivity is much lower than that of the electrode spacer. Electrothermal waves tend to propagate in z direction under large Hall parameters, as pointed out in Ref. 3. However, the critical current density for the initiation of constrictions do not differ much from those evaluated under the condition $k_z = 0$ for the Hall parameter range adopted in open-cycle MHD power generation. For this reason, we also assume $k_z = 0$ in the following calculations.

With the above conditions, $P_0 = P_2 = 0$ in Eq. (6) and the current amplitude can be obtained as,

$$J_{ym} = \frac{k_x^2(1+\beta_y^2+\beta_z^2)}{k_x^2+(1+\beta_y^2)(m\pi/\delta)^2} \frac{J_{y0}\sigma_T A_m}{(1+\beta_y^2)} \sin\left(\frac{m\pi y}{\delta}\right)$$

$$= B_m \sin\left(\frac{m\pi y}{\delta}\right) \tag{13}$$

Performing the integration of Eq. (10), we obtain

$$\langle m|n\rangle = \langle m|m\rangle = B_m^2\left(\frac{\delta}{2}\right)\left\{\left[\left(\frac{m\pi}{\delta}\right)^4 + Q_0\left(\frac{m\pi}{\delta}\right)^2 + S_0\right]^2 - R_0^2\left(\frac{m\pi}{\delta}\right)^2\right\} \tag{14}$$

where $\langle m|n\rangle = 0$ in case $m \neq n$ and Q_0, R_0, and S_0 are given by

$$Q_0 = \frac{k_x^2}{(1+\beta_y^2)} + \frac{i\omega}{\alpha_0} - \frac{ik_xV}{\alpha_0} + k_x^2 + \frac{(1+\beta_y^2)a_y^2/(1+\beta_y^2+\beta_z^2)}{(\alpha_0\rho_0C_p\sigma_0\sigma_T)}$$

$$R_0 = \frac{2\beta_z a_y^2 k_x/(1+\beta_y^2+\beta_z^2)}{(\alpha_0\rho_0C_p\sigma_0\sigma_T)}$$

$$S_0 = \frac{k_x^2(i\omega/\alpha_0 - ik_xV/\alpha_0 + k_x^2)}{(1+\beta_y^2)} - \frac{a_y^2k_x^2/(1+\beta_y^2+\beta_z^2)}{(\alpha_0\rho_0C_p\sigma_0\sigma_T)}$$

Therefore, Eq. (11) requires that

$$\prod_{m=1}^{\infty}\left\{\left[\left(\frac{m\pi}{\delta}\right)^4 + Q_0\left(\frac{m\pi}{\delta}\right)^2 + S_0\right]^2 - R_0^2\left(\frac{m\pi}{\delta}\right)^2\right\} = 0$$

and the dispersion relation can be obtained as follows:

$$\frac{1}{\alpha_0}\mathrm{Im}\omega = \left(\frac{m\pi}{\delta}\right)^2 + k_x^2 - \frac{\sigma_T J_{0y}^2}{\alpha_0\rho_0C_p\sigma_0}\frac{1+\beta_y^2+\beta_z^2}{1+\beta_y^2}$$

$$\times\frac{k_x^2+2(m\pi/\delta)\beta_z k_x - (1+\beta_y^2)(m\pi/\delta)^2}{(1+\beta_y^2)(m\pi/\delta)^2+k_x^2} \tag{15}$$

Table 1 Ranges of magnetic field and Hall's parameter near electrodes of a SFC-type MHD generator

Design	y component	z component
Ferromagnetic wall		
B, T	1.0-1.2	0.2-0.6
β	0.3-0.35	0.1-0.3
Superconducting magnet		
B, T	2.0-3.0	0.2.0
β	0.57-0.87	0.-1.0

where $m = 1,2,\ldots$. Note that the real part of the frequency is given by $\mathrm{Re}\omega = k_xV$, so that the fluctuations travel in x direction with a phase speed equal to the flow velocity.

As the perturbation becomes unstable if $\mathrm{Im}\omega < 0$, the stability limits are obtained by equating $\mathrm{Im}\omega$ to zero as follows:

$$\frac{\sigma_T J_{0y}^2}{\alpha_0\rho_0C_p\sigma_0} = \frac{1+\beta_y^2}{1+\beta_y^2+\beta_z^2}$$

$$\times\frac{[(m\pi/\delta)^2+k_x^2][(1+\beta_y^2)(m\pi/\delta)^2+k_x^2]}{k_x^2+2(m\pi/\delta)\beta_z k_x - (1+\beta_y^2)(m\pi/\delta)^2} \tag{16}$$

This relation clearly indicates that the increase in the Hall parameter β_z decreases the stability limit and the increase in β_y increases the limits significantly. In the uniform B-field generator, β_y is zero. Therefore, increase in the magnetic field strength always decreases stability limits. In the shaped B-field generator, however, the existence of B_y component provides the possibility to increase the stability limit even under a high B-field imposed in the core region. We can evaluate β_y and β_z in the SFC-type generator as follows. The shaped B-field configuration can be realized by a ferromagnetic wall design[10] in the case of an iron-cored magnet and by an appropriate design of both the generator electrode and the coil positions[11] in the case of a superconducting magnet. Examples of the B-field distribution in both design cases are shown in Fig. 2. In both cases, the y component is zero at the center of the electrode ($y = 0$ and D, $z = 0$) and it has a maximum value B_{ym} at the corner of the cross section ($y = 0$ and D, $z = \pm W/2$). Assuming roughly a parabolic distribution for $B_y^2(z)$ on the electrode surface, we evaluate B_y by an average as $\bar{B}_y^2 = B_{ym}^2/3$. For the ferromagnetic wall design, it is easy to realize $B_{ym} \simeq 1.2$ T, and $B_{zw} \simeq 0.2 \sim 0.6$ T on the surface, and for the superconducting magnet case, $B_{ym} \simeq 2 \sim 3$ T and $B_{zw} \simeq 0 \sim 2$ T. Employing these values and $\mu_0 = 0.5$ m$^2 \cdot V^{-1} \cdot$s^{-1}, we estimate the ranges of Hall parameters near electrode walls of the SFC-type generator, as shown in Table 1. The core plasma Hall parameter, which is also the Hall parameter for the uniform B-field generator, is up to about $\beta_z \simeq 2$ in the iron-cored magnet and $\simeq 4$ in a superconducting magnet.

Figure 3 depicts the dimensionless stability limits defined by $\bar{A} = \sigma_T\delta^2 J_{0y}^2/(\alpha_0\rho_0C_p\sigma_0\pi^2)$ vs the dimensionless wave number $\bar{k}_x = k_x\delta/\pi$ for each $m = 1$ and 2 constriction mode. In the region above each curve, the perturbations are unstable and the minimum point of each curve defines the critical conditions for $\bar{A}$ and $\bar{k}_x$. From these results, it is concluded that the $m = 1$ mode is most likely to occur in the magnetohydrodynamic plasma and, if the perturbation is stable for this primary mode, then the equilibrium current transfer process is always stable for higher-constriction modes.

The ranges between the curves a-a′ and b-b′ correspond to both the ferromagnetic wall design and the superconducting magnet design cases in the SFC-type MHD generator, respectively. It is shown in the figures that the stability limits of the UFC-type are strongly decreased with the increase in the Hall parameter β_z. In an open-cycle MHD generator, the turbulent heat transfer seems to be dominant. Assuming a core velocity 800 m$\cdot$s^{-1} and the turbulent boundary layer thickness to be 5×10^{-2} m, we evaluate the displacement thickness to be about one-tenth of this thickness and the turbulent thermal diffusivity $\alpha_t \simeq 7.5 \times 10^{-2}m^2 \cdot$s^{-1}. The turbulent arc-layer thickness may be one order thicker than that of the laminar arc-layer, e.g., $\delta \simeq 10^{-2}$ m. So that with $T_0\sigma_T \simeq 13$, $T_0 \simeq 1.5 \times 10^3$ K, $\sigma_0 \simeq 1$ S$\cdot$m^{-1}, and $\rho_0 \simeq 0.2$ kg$\cdot$m^{-3}, then $\bar{A} \simeq 0.1 \sim 1$ for $J_{0y} = 0.5 \times 10^4 \sim 10^4A\cdot$m^{-2}. In Fig. 3a, it is seen that, in the uniform B-field case, the plasma is unstable for this range of the $\bar{A}$ values under Hall parameters larger than 2. On the contrary, in the shaped B-field case, the $\bar{A}$ values evaluated above are within the stable region for all Hall's parameters $\bar{\beta}_y$ and β_{zw}. It is to be noted that, in the superconducting magnet regime (curve b), the stability limit

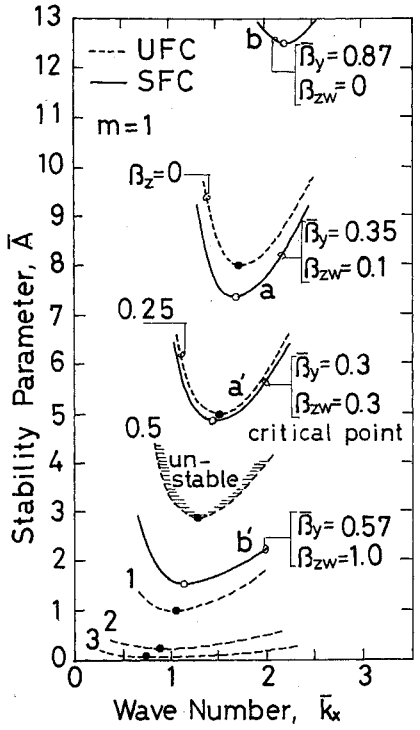

Fig. 3a Stability limits of $m=1$ mode electrothermal waves near electrically nonconductive and thermally conductive electrodes for various Hall parameters in both the UFC- and SFC-type MHD channels.

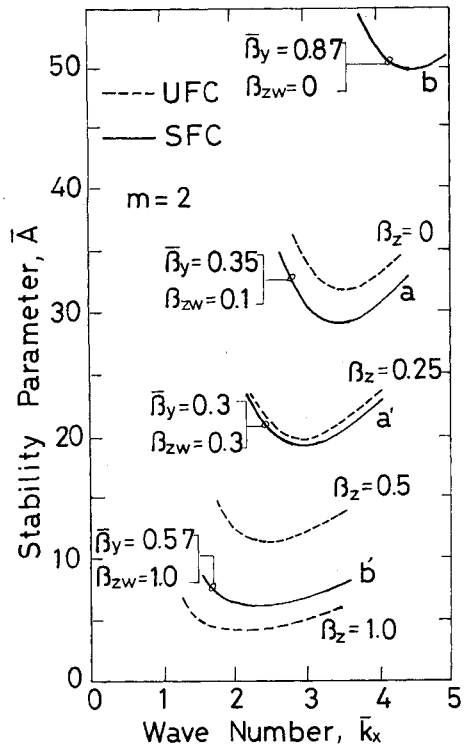

Fig. 3b Stability limits of $m=2$ mode electrothermal waves under the same surface conditions as Fig. 3a.

for $\beta_z=3$ for the UFC type can be improved by factors of 100, namely, the stable current density limit may be improved by factors of 10.

The current constriction may actually occur under the critical condition defined by the minimum point of each curve. These $\bar{A}_{cr}$ are plotted in Fig. 4 for the UFC and SFC types and the corresponding wave number $\bar{k}_{xcr}$ in Fig. 5, respectively. Figure 4 shows that the critical current density J_{0y}, which is

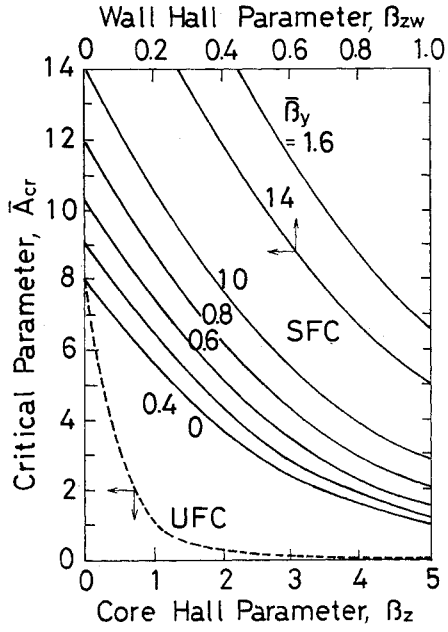

Fig. 4 Critical parameter $\bar{A}_{cr}$ for various Hall's parameters β_z (UFC), and β_{zw} and $\bar{\beta}_y$ (SFC) for the case shown in Fig. 3a.

proportional to $\sqrt{A_{cr}}$ is higher in the SFC type than in the UFC type by factors of 5-10. We can see that the design of the magnetic field configuration yielding a low β_{zw} as well as a high β_y is extremely useful for the stabilization of current transport processes. Figure 5 shows that, even when the constrictions occur in the SFC type, the critical wave number is larger than in the UFC type by a factor of two, so that the wavelength (that is, the number of arc spots per unit length of the electrode) may be doubled and the current per arc spot is about one-half of that of the uniform B-field MHD channel.

Thermally and Electrically Conductive Electrode

Here, we consider the case of a cooled clean metal electrode. The boundary conditions for this thermally and electrically conductive surface are

$$\hat{T}(0)=\hat{T}(\delta)=\hat{E}_x(0)=\hat{J}_y(\delta)=0$$

Again, we consider two-dimensional wave ($k_z=0$) in the $m=1$ mode under the conditions: $\epsilon_{0x}=\epsilon_{0z}=0$. Assuming the same solution for the temperature perturbation [Eq. (12)], we obtain $J_{y1}(y)$ as

$$J_{y1}=B_1\{\sin(\pi y/\delta)-K_a\sinh[\sqrt{P_1}(y-\delta)] - iK_b\sinh[\sqrt{P_1}(y-\delta)]\} \tag{17}$$

where

$$B_1=A_1k_x^2a_y/[(\pi/\delta)^2(1+\beta_y^2)+k_x^2]$$

$$P_1=k_x^2/(1+\beta_y^2)$$

$$K_a=\frac{(\pi/\delta)\cosh(\sqrt{P_1}\delta)}{\sqrt{P_1}[\cosh^2(\sqrt{P_1}\delta)+\beta_z^2\sinh^2(\sqrt{P_1}\delta)/(1+\beta_y^2)]}$$

$$K_b=\frac{(\pi/\delta)\beta_z\sinh(\sqrt{P_1}\delta)}{k_x[\cosh^2(\sqrt{P_1}\delta)+\beta_z^2\sinh^2(\sqrt{P_1}\delta)/(1+\beta_y^2)]}$$

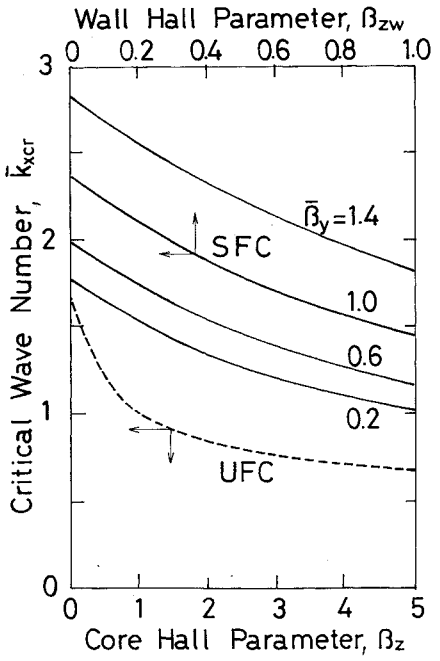

Fig. 5 Critical wavenumber dependence upon the Hall parameter for the case shown in Fig. 3a.

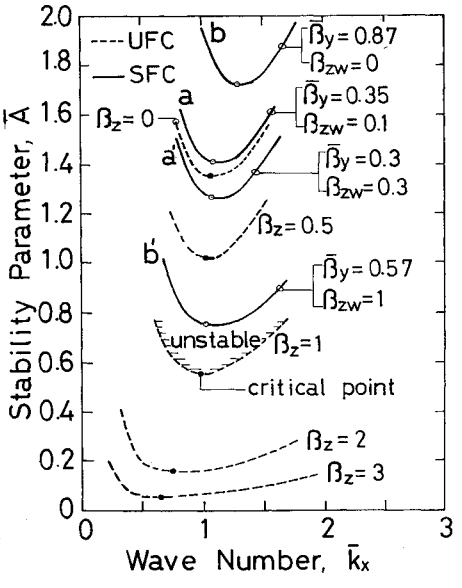

Fig. 6 Stability limits of electrothermal waves ($m=1$) near electrically and thermally conductive electrodes.

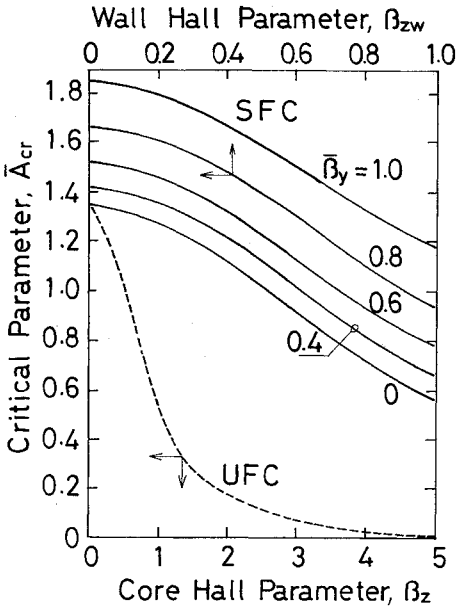

Fig. 7 Critical parameters $\bar{A}_{cr}$ for various Hall parameters β_z, β_{zw}, and $\bar{\beta}_y$ for the case shown in Fig. 6.

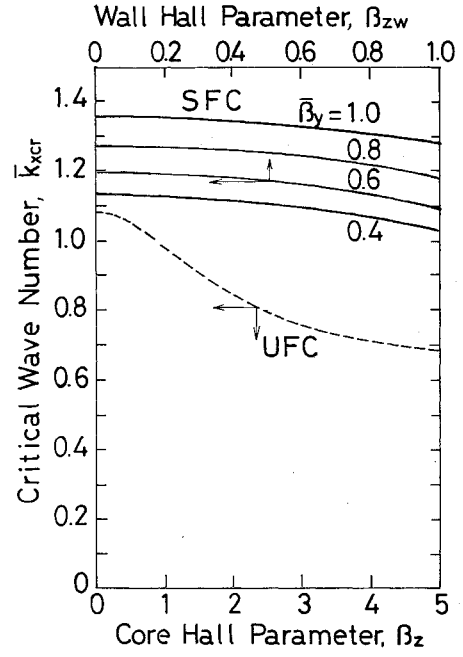

Fig. 8 Critical wavenumber dependence upon the Hall parameters β_z, β_{zw}, and $\bar{\beta}_y$ for the case depicted in Fig. 6.

Carrying out the integration of Eq. (10) with $m=n=1$, we obtain the dispersion relation as

$$X^2+2\left[\left(\frac{\pi}{\delta}\right)^2+\frac{(\pi/\delta)^2-P_1-\theta_1P_1}{(\pi/\delta)^2+P_1}\,\frac{(1+\beta_y^2+\beta_z^2)A}{(1+\beta_y^2)}\right]X$$
$$+\left(\frac{\pi}{\delta}\right)^4+\theta_1P_1^2+\frac{2[(\pi/\delta)^4-P_1(\pi/\delta)^2+\theta_1P_1^2]}{(\pi/\delta)^2+P_1}$$
$$\times\frac{(1+\beta_y^2+\beta_z^2)A}{1+\beta_y^2}+\left[1-\frac{4P_1(1+\beta_y^2+\beta_z^2)}{1+\beta_y^2}\right.$$
$$\left.\times\frac{(\pi/\delta)^2+\theta_2P_1-\theta_1P_1}{[(\pi/\delta)^2+P_1]^2}\right]\frac{(1+\beta_y^2+\beta_z^2)^2A^2}{(1+\beta_y^2)^2}=0 \qquad (18)$$

where the following substitutions have been made:

$$X=i\omega/\alpha_0-ik_xV/\alpha_0+k_x^2$$

$$A=\sigma_TJ_{0y}^2/(\alpha_0\rho_0C_p\sigma_0)$$

$$\theta_1=4(\pi/\delta)^2\sinh(\sqrt{P_1}\delta)\cosh(\sqrt{P_1}\delta)/[\cosh^2(\sqrt{P_1}\delta)$$
$$+\beta_z^2\sinh^2(\sqrt{P_1}\delta)/(1+\beta_y^2)]/[(\pi/\delta)^2+P_1]/(\sqrt{P_1}\delta)$$

$$\theta_2=(\pi/\delta)^2[\sinh(\sqrt{P_1}\delta)\cosh(\sqrt{P_1}\delta)/(\sqrt{P_1}\delta)+1]$$
$$\div[1+(1+\beta_y^2+\beta_z^2)\sinh^2(\sqrt{P_1}\delta)/(1+\beta_y^2)]/P_1$$

The stability limit is obtained by equating Imω to zero and Re$\omega = k_x V$ in Eq. (18), which can be reduced to the following quadratic form with respect to A.

$$\phi_1 A^2 - 2\phi_2 A - \phi_3 = 0 \tag{19}$$

where

$$\phi_1 = \left\{ 4P_1 \frac{[(\pi/\delta)^2 + \theta_2 P_1 - \theta_1 P_1](1+\beta_y^2+\beta_z^2)}{[(\pi/\delta)^2 + P_1]^2/(1+\beta_y^2)} - 1 \right\} \times \frac{(1+\beta_y^2+\beta_z^2)^2}{(1+\beta_y^2)^2}$$

$$\phi_2 = \left\{ \left[\left(\frac{\pi}{\delta}\right)^2 - P_1 - \theta_1 P_1 \right] k_x^2 + \left(\frac{\pi}{\delta}\right)^4 - P_1 \left(\frac{\pi}{\delta}\right)^2 + \theta_1 P_1 \right\} \times \frac{(1+\beta_y^2+\beta_z^2)/(1+\beta_y^2)}{(\pi/\delta)^2 + P_1}$$

$$\phi_3 = [(\pi/\delta)^2 + k_x^2]^2 + \theta_1 P_1^2$$

Solving Eq. (19), we obtain the stability limit A as

$$A = [1 + \sqrt{1 + \phi_1\phi_3/\phi_2^2}]\,\phi_2/\phi_1 \tag{20}$$

It can be shown numerically that the other root of Eq. (19) is physically meaningless ($A < 0$).

Normalized stability limits are plotted in Fig. 6 with the same Hall parameter ranges used in the previous section for both the UFC and the SFC cases. The critical values $\bar{A}_{cr}$ and the corresponding critical wave number $\bar{k}_{xcr}$ are shown in Figs. 7 and 8, respectively.

We note that the stability limits for low Hall's parameter ranges are very small in this case in comparison with those evaluated in the preceding section. However, $\bar{A}_{cr}$ and $\bar{k}_{xcr}$ for a high Hall's parameter ($\beta_z \geq 2$) are not much different from those shown in Figs. 3-5. Thus, from a practical viewpoint, the arc transition characteristics near an electrically and thermally conductive electrode are almost the same as in the case of electrically nonconductive and thermally conductive electrodes. Also, it should be noted that the stability limits of the UFC-type MHD generator can also be greatly improved in the SFC type in both the ferromagnetic wall design (a-a′) and the superconducting magnet design ranges (b-b′). As seen in Fig. 7, the increase in $\bar{\beta}_y$ as well as the decrease in β_{zw} near electrodes is comparably useful for the increase in the critical current density.

Conclusions

Based on the variational calculus, a general dispersion relation for electrothermal waves in a weakly ionized magnetohydrodynamic plasma was obtained with taking into account three components of both the electric field and the current density under an applied magnetic field with two components. Using the general criterion, we calculated the stability limits for two typical electrode surface conditions in the open-cycle MHD generator. We showed evidence that the shaped B-field configuration with reduced B_z and moderate B_y components in the region near electrode walls significantly relaxed the critical conditions for typical diffused to arc transition phenomena in an MHD generator. The critical current densities under the shaped B-field configuration are higher than those under the uniform B-field by about 5-10. This conclusion may hold for both the laminar and turbulent boundary-layer models, because steady-state thermal properties in the boundary layers are approximately the same under two different magnetic field configurations and the ratio of the critical current density of the SFC to that of the UFC is determined independently of the thermal diffusivities.

Nonuniformities in the steady-state temperature and the magnetic field in the SFC case have not been considered in the present paper. These assumptions do not introduce significant errors in the case of a thin-arc-layer model. However, effects of varying these properties in the case of a thick arc layer (order of 10^{-2}m) are unclear. Extensions of the present work in this respect will be reported later.

Appendix

The Euler equation with $n = 4$ is

$$[D^8 + (P_0^2 - 2Q_0)D^6 + (Q_0^2 + 2P_0R_0 + 2S_0)D^4 + (R_0^2 - 2Q_0S_0)D^2 + S_0^2]\,\hat{J}_y(y) = 0 \tag{A1}$$

Thus, the action integral should be written as

$$I[\hat{J}_y(y)] = \int_0^\delta [(D^4\hat{J}_y)^2 - (P_0^2 - 2Q_0)(D^3\hat{J}_y)^2 + (Q_0^2 + 2P_0R_0 + 2S_0)(D^2\hat{J}_y)^2 - (R_0^2 - 2Q_0S_0)(D\hat{J}_y)^2 + S_0^2\hat{J}_y^2]\,dy \tag{A2}$$

Assuming

$$\hat{J}_y(y) = \sum_{m=1}^{\infty} A_m J_{ym}(y)$$

is inserted into the above integral, we get Eq. (9), which should be an extreme with respect to $\hat{J}_y$, namely A_m. This requires that

$$\sum_{n=1}^{\infty} A_n \langle m|n\rangle = 0 \quad \text{for } m = 1,2,\ldots$$

Acknowledgments

The author would like to acknowledge the useful discussions held with Y. Aoki and S. Oikawa. He also thanks Profs. H. Yamazaki and Y. Ogawa for their encouraging support during the course of this work. This work was sponsored by the Energy Conversion Research Institute of Hokkaido University.

References

[1]Khait, V.D., "A Model for Formation of Anodal Spots on Hot Electrodes in a Weakly Ionized Molecular Plasma Stream," *High Temperature,* Vol. 15, No. 3, 1977, pp. 418-425.

[2]Oliver, D.A., "A Constricted Discharge in Magnetohydrodynamic Plasma," *Proceedings of 15th Symposium on Engineering Aspects of MHD,* Univ. of Pennsylvania, May 1976, p. IX.4.1.

[3]Okazaki, K., Mori, Y., Hijikata, K., and Ohtake, K., "MHD Boundary Layer of the Seeded Combustion Gas Near Cold Electrodes," *AIAA Journal,* Vol. 18, Jan. 1980, pp. 43-46.

[4]Kon, T., Kayukawa, N., Aoki, Y., and Ozawa, Y., "Electrical and Thermal Instabilities in the Electrode Surface Region in a Combustion MHD Generator Channel," *Proceedings of 16th Symposium on Engineering Aspects of MHD,* Univ. of Pittsburgh, May 1977, p. VI.1.1.

[5]Kayukawa, N., Aoki, Y., Ozawa, Y., Yoshida, M., and Umoto, J., "Electrical Characteristics of an MHD Generator with a Transversally Shaped Configuration of Magnetic Induction," *Journal of Energy,* Vol. 7, May-June 1983, pp. 280-284.

[6]Eckert, E.R.G. and Drake, R. Jr., *Analysis of Heat and Mass Transfer,* McGraw-Hill Book Co., New York, 1972, p. 363.

[7]Okazaki, K., Mori, Y., Hijikata, K., and Ohtake, K., "Electrothermal Instability in the Seeded Combustion Gas Boundary Layer near Cold Electrodes," *AIAA Journal,* Vol. 16, April 1978, pp. 334-339.

[8]Kayukawa, N., Oikawa, S., Aoki, Y., Yamazaki, H., and Ozawa, Y., "Electrothermal Instability Analysis for an Open-Cycle MHD Plasma under Two-Component Magnetic Field," *Proceedings of 22nd Symposium on Engineering Aspects of MHD,* Mississippi State Univ., June 1984, p. 5.2.10.

[9]Courant, R. and Hilbert, D., *Methods of Mathematical Physics,* 4th ed., Vol. 1, Wiley-Interscience, New York, 1963, p. 190.

[10]Kayukawa, N. and Ozawa, Y., U.S. Patent, No. 4 218 629, Aug. 19, 1980.

[11]Kayukawa, N., Oikawa, S., Aoki, Y., and Ozawa, Y., "Transversally Shaped Field Configuration and Output Performance Evaluation for Slagged Rectangular MHD Channel with Superconducting Coil System," *Proceedings of Eighth International Conference on MHD Electrical Power Generation,* Vol. 2, Sept. 1983, pp. 78-82.